DEVELOPMENTAL DYNAMICS 201:29–40 (1994)

Time-Lapse Total Internal Reflection Fluorescence Video of Acetylcholine Receptor Cluster Formation on Myotubes

MICHELLE DONG WANG AND DANIEL AXELROD
Biophysics Research Division (M.D.W., D.A.) and Department of Physics (D.A.), University of Michigan, Ann Arbor, Michigan 48109

ABSTRACT **To study when and where acetylcholine receptor (AChR) clusters appear on developing rat myotubes in primary culture, we have made time-lapse movies of total internal reflection fluorescence (TIRF) overlaid with schlieren transmitted light images. The receptors, including the ones newly incorporated into the membrane, were labeled with rhodamine α-bungarotoxin (R-BT) continuously present in the medium. Since TIRF illuminates only cell-substrate contact regions where almost all of the AChR clusters are located, background fluorescence from fluorophores either in the bulk solution or inside the cells can be suppressed. Also, because TIRF minimizes the exposure of the cell interior to light, the healthy survival of the culture during imaging procedures is much enhanced relative to standard epi- (or trans-) illumination. During the experiment, cells were kept alive on the microscope stage at 37°C in an atmosphere of 10% CO_2. Two digital images were recorded by a CCD camera every 20 min: the schlieren image of the cells and the TIRF image of the clusters. After background subtraction, the cluster image was displayed in pseudocolors, overlaid onto the cell images, and recorded as 3 frames on a videotape. The final movies are thus able to summarize a week-long experiment in less than a minute. These movies and images show that clusters form often shortly after the myoblast fusion but sometimes much later, and the formation takes place very rapidly (a few hours). The clusters have an average lifetime of around a day, much shorter than the lifetime of a typical myotube. The brightest and largest clusters tend to be the longest-lived. The cluster formation seems to be associated with the contacts of myotubes at the glass substrate, but not with cell-cell contacts or myoblast fusion into myotubes. New AChR continuously appear in preexisting clusters: after photobleaching, the fluorescence of some clusters recovers within an hour.**

Key words: Rat muscle, CCD imaging, Synaptogenesis, α-bungarotoxin, Schlieren optics, Contact regions

INTRODUCTION

Clustering of acetylcholine receptors (AChRs) at the postsynaptic membrane is a critical event during the early development of the neuromuscular junction (Block and Pumplin, 1988; Changeux, 1989; Changeux et al., 1989; Kuromi, 1987). However, the mechanism of the clustering is not well understood on the molecular level. On rat muscle cells, previous studies have shown that the clustering not only occurs at the neuromuscular synapses (in vivo) but also can be induced in culture (in vitro) by contact with the substrate, nerves, or basic polypeptide-coated latex beads; or by supplementing the medium with embryonic brain extract, basal lamina extract, or basic fibroblast growth factor (Froehner, 1991; Krikorian and Daniels, 1989; Olek et al., 1986). The AChR clusters in vitro have served as convenient model systems for understanding the mechanisms of clustering in vivo.

One system widely used is the clusters induced by substrate-contact in aneural myotube cultures (e.g., Bloch et al., 1989). The in vitro AChR clusters in the aneural myotube cultures resemble those of in vivo neuromuscular junctions in their morphology and in their associations with intracellular and extracellular components (Froehner, 1991; Bloch et al., 1989). In particular, both types are shown to be directly associated with cytoplasmic aggregations of 43K protein, and are speculated also to be directly associated with actin and β-spectrin (Froehner, 1991). However, the in vitro clusters appear to be more dynamic, appearing and then disappearing in a matter of days or less, with an even more rapid turnover of individual AChR within a cluster.

AChR clusters can be easily visualized in a fluorescence microscope by treatment with tetramethylrhodamine-labeled α-bungarotoxin (R-BT). Because of certain technical difficulties involving background fluorescence and cell deterioration under illumination, the life cycle of clusters has not been previously described in detail. The main point of this study is to overcome those difficulties by utilizing total internal

Received January 13, 1994; accepted May 16, 1994.
Address reprint requests/correspondence to Daniel Axelrod, Biophysics Research Division, University of Michigan, 930 N. University, Ann Arbor, MI 48109.

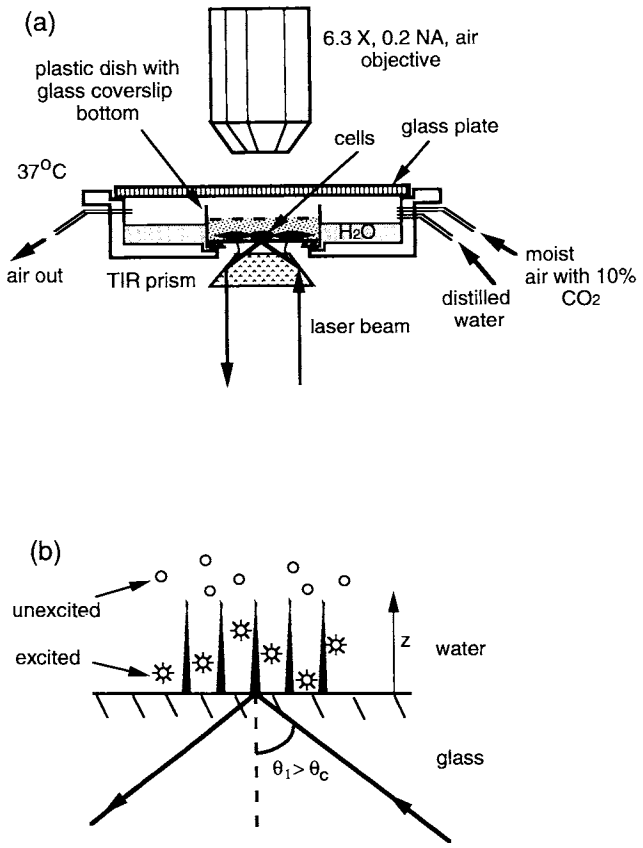

Fig. 1. (**a**) The cell growth chamber and surrounding optics. The cell growth chamber was designed to fit onto an upright microscope stage with TIRF illumination. The AChRs were labeled with R-BT which was continuously present in the medium, and were excited by a TIR laser beam through a trapezoidal prism mounted on the microscope condenser holder from below. The culture dish was sealed into a groove around the bottom hole of the chamber with high vacuum grease. The chamber was covered by a 50 × 75 mm standard glass slide also sealed to the chamber with high vacuum grease. The culture dish was stabilized by two thin stacks of Scotch tape placed in between the edge of the dish and the chamber cover, and the cover was secured with two springs screwed onto the chamber top. To prevent water loss in the cell culture medium due to evaporation, the chamber was filled with distilled water around the culture dish through the water refill port to keep the air inside moisturized. The 10% CO_2 atmosphere was also passed through a moisturizer before being sent into the air entry port. To prevent fungus and bacteria from growing in the culture, each component of the chamber was thoroughly cleaned with 70% EtOH, rinsed with distilled water, and sterilized under a UV light hood before the cell culture dish was mounted into the chamber. This sterilization was later maintained on the microscope stage since both the 10% CO_2 atmosphere and the distilled water were passed through sterile acrodisc syringe filters before they entered the chamber. The temperature of the chamber was kept at 37°C by an air blower/heater (Arenberg Sage, Jamaica Plain, MA) with its temperature sensor attached to the bottom of the chamber. (**b**) Principles of TIRF. When light travels from a high refractive index medium of refractive index n_2 to a low refractive index medium of refractive index n_2, it undergoes total internal reflection if incidence angle Θ_1 is greater than the critical angle Θ_c. An exponentially decaying "evanescent wave" propagates parallel to the surface in the low refractive index medium. Only fluorophores in this field will be excited. In this study, these fluorophores consist almost exclusively of R-BT bound to AChR in the portion of myotube membrane near the substrate. Other R-BT molecules free in solution and most intrinsic cytoplasmic fluorophores remain unexcited since they lie outside the evanescent wave depth.

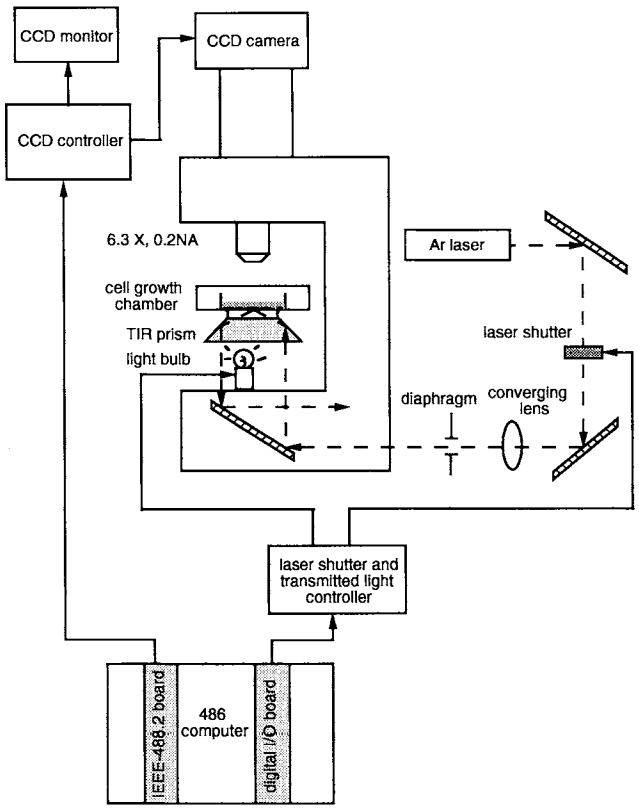

Fig. 2. The image acquisition setup. The process of image acquisition is designed to be completely automated through the computer using a FORTRAN/assembly language program. The cells and their AChR clusters are observed sequentially by alternating the schlieren transmitted light illumination and TIRF. The controllers for the transmitted light, the laser shutter, and the CCD camera are all interfaced to the computer.

reflection fluorescence (TIRF). TIRF illuminates only the cell-substrate contact regions; AChR clusters on rat myotubes happen to reside almost exclusively in such regions.

In order to study when and where in vitro clusters form on myotubes, we have made time-lapse TIRF movies of AChR cluster formation on developing rat myotubes in primary cultures. This is the first time-lapse TIRF sequence recorded on any biological system, and the technique offers numerous generally applicable advantages to be discussed. The AChRs were labeled with R-BT which was continuously present in the medium. The TIRF images of the AChR clusters were overlaid on top of the images of the cells produced by schlieren transmitted light optics. Both of the observations were made every 20 min and recorded as digital images using a charge coupled device (CCD) camera. The final movie thus condenses a week-long experiment into less than a minute. This system offers a far more detailed, extensive, and frequent view of the progress of individual clusters than sequences of still photographs taken with conventional fluorescence epi-illumination (e.g., Krikorian and Daniels, 1989).

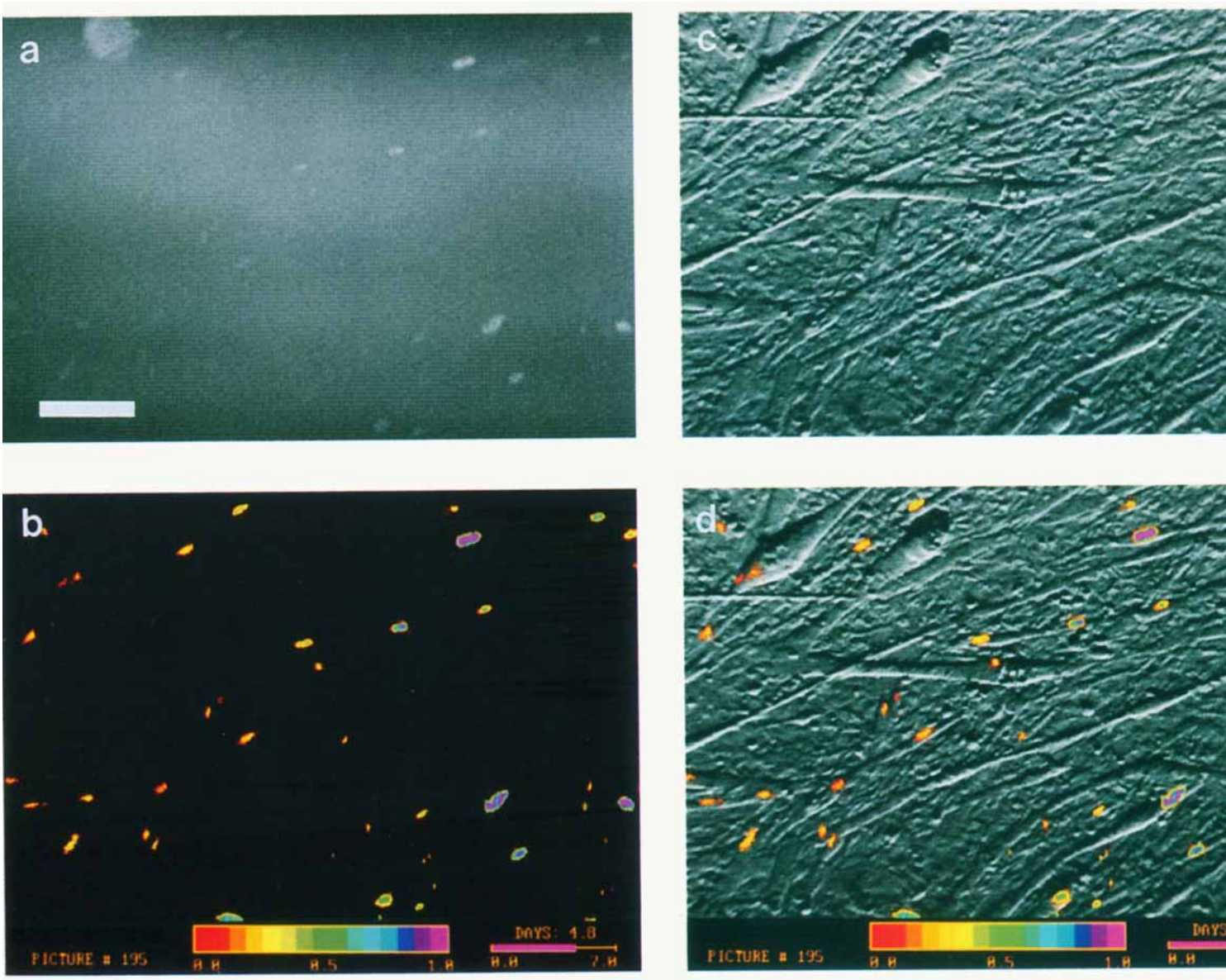

Fig. 3. Stages of image processing. (**a**) The original TIRF cluster image. The bright spots are clusters except the one which is debris at the upper left-hand corner. The range of grey levels here is somewhat reduced from the original image. (**b**) Cluster image after background subtraction and pseudocoloring. (**c**) The *schlieren illumination cell image*. (**d**) Overlay of (b) onto (c). The color bars in (b) and (d) represent cluster intensities from dim as red to bright as purple. Bar = 100 μm.

MATERIALS AND METHODS

Rat Muscle Cell Culture Preparation

To minimize the autofluorescence from the substrate, the standard disposable plastic culture dish (35 × 10 mm) was modified by drilling a 7/8 inch diameter hole in the bottom and gluing in a standard 25 mm circular no. 1 glass cover slip. Cells were plated directly into such dishes without any precoating.

Tetramethylrhodamine α-bungarotoxin (R-BT) was prepared as described previously (Ravdin and Axelrod, 1977) from unlabeled α-bungarotoxin (Biotoxins, St. Cloud, FL) and 5′-(and 6′-) carboxytetramethylrhodamine, succinimidyl ester (Molecular Probes, Eugene, OR).

A detailed description of the culture preparation can be found in Axelrod (1980) and Bloch (1979). In brief, rat muscle cell cultures were prepared from the hind leg skeletal muscle tissues of neonatal rats. These cells were initially plated in 2 ml of culture medium (consisting of Dulbecco's modified Eagle medium + 10% fetal calf serum + 0.5% penicillin-streptomycin, all from Grand Island Biological Co., Grand Island, NY) in modified culture dishes, and were then grown in an incubator at 37°C in 7% CO_2 atmosphere mixture. After 1–2 days, R-BT was added to the 2 ml of cell medium to achieve a final concentration of about 4 μg per ml. The fluorophores in the medium serve as a continuous reservoir to label the receptors that are newly incorporated into the cell membranes. The culture dish was then transferred into a cell growth chamber custom-designed for use on the upright microscope (Leitz Ortholux II) stage.

The cell growth chamber shown and described in Figure 1a was specially designed to be airtight with ports (made of syringe needles) for a 10% CO_2 atmosphere mixture flow-through for use on the microscope stage.

Total Internal Reflection Fluorescence (TIRF) and Schlieren Optics

TIRF (Axelrod et al., 1984, 1992) is a technique for studying molecular and cellular phenomena at liquid/solid interfaces. When light travels from a high refractive index medium of refractive index n_1 to a low refractive index medium of refractive index n_2, it undergoes total internal reflection (TIR) if the incidence angle Θ_1 is greater than the critical angle Θ_c as shown in Figure 1b. The critical angle is defined by

$$\Theta_c = \sin^{-1}(n_2/n_1) \quad (1)$$

In the lower refractive index medium, a so-called evanescent wave propagates parallel to the interface in the incidence plane and its intensity decays exponentially with increasing distance z from the interface with a characteristic decay distance *d:*

$$I(z) = I(0)e^{-z/d} \quad (2)$$

where

$$d = \frac{\lambda_o}{4\pi}(n_1^2 \sin^2 \theta_1 - n_2^2)^{-1/2}. \quad (3)$$

λ_o is the wavelength of the light in vacuum.

In our optical setup (see Fig. 1a), a trapezoidal prism mounted on the microscope's condenser carrier is brought into optical contact (via immersion oil) with the bottom surface of the glass coverslip upon which the cells grow. The excitation laser beam (λ_o = 514.5 nm) is directed to the trapezoidal prism's top surface at an incidence angle of 60° (>Θ_c) by the trapezoidal prism. The evanescent field emerges in the culture medium near the interface where it excites the fluorescently labeled AChR clusters which are proximal to this interface. The characteristic exponential decay depth (d) of the evanescent field given by Equation (3) is d = 21.2 nm. (Labeled AChR residing at a distance of 2 d from the substrate would thereby fluoresce with only e^{-2} of the intensity of labeled AChR immediately at the substrate surface.) This depth (d) is much smaller than the width of a typical myotube (20 μm), but larger than the thickness of plasma membrane bilayer (~4.5 nm), or the thickness of plasma membrane taking the membrane proteins into account (~15 nm) (Haest, 1982). R-BT labeled AChR clusters can therefore be visualized with very little background fluorescence from fluorophores either in the bulk solution or inside of the cells, and with minimal photodamage to the cells.

The source of TIRF illumination was an argon laser with an output power of less than 100 mW. The area of TIRF illumination was a stripe with a length greater than the field of view and a width that was narrowed to approximately the width of the field of view by a converging lens positioned before the trapezoidal prism. With this area of illumination and with losses in the illumination optics of the system, we estimate the illumination intensity to be less than 5 nW/μm^2.

The positions and shapes of the cells were observed using schlieren transmitted light microscopy. Schlieren optics produces image intensities sensitive to phase gradients in the sample (Axelrod, 1981). In this application, it was created simply by placing a light bulb below the TIRF trapezoidal prism and slightly off center.

Light Detection

Both the transmitted light and the fluorescence were collected by a 6.3×, N.A. 0.2, air-immersion objective. (This relatively low power objective was used to enable viewing of a large field.) The alternation of the schlieren transmitted light microscopy and TIRF was controlled electronically by the transmitted light and laser shutter controller especially designed to be interfaced to an I486/50 MHz computer through a digital I/O board (Metrabyte CTM-05) (see Fig. 2). The images were recorded digitally using a CCD camera (Photometrics Star I, Photometrics, Inc., Tucson, AZ) and displayed on a CCD monitor. The CCD camera controller

was also interfaced to the computer through an IEEE-488.2 board.

A custom Fortran/assembly language program which called commercial subroutines for operating the CCD camera automated the following controls and data acquisition functions: turning the schlieren transmitted light source on and off; opening and closing the TIRF laser source shutter; setting the exposure times of the CCD camera; opening and closing the camera shutter; and reading CCD images from the CCD controller. During the experiment, 2 images were taken every 20 min, one for the cells with the schlieren transmitted light, and the other for the clusters with TIRF. The duration of illumination was 1 sec for TIRF and 6 sec for schlieren optics; and the durations of light collection were 0.3 sec for TIRF and 3 sec for schlieren optics. Both images were recorded digitally onto the computer hard disk, and later transferred to a magnetic tape.

Image Processing

A CCD image has a dimension of 576 × 384 (column × row) pixels, and a maximum pixel intensity of 12 bits. It is recorded as a 442,368 byte binary file with the intensity of each pixel recorded in 16 bits. A custom-designed image processing procedure works on these files and serves to eliminate background fluorescence from the TIRF cluster image, add text captions, pseudocolor the clusters according to pixel intensity, and overlay the TIRF cluster image on top of the schlieren cell image. Figure 3a–d shows a typical scene in a myotube culture as it progresses through our image processing sequence and is displayed on a VGA computer monitor.

The conventional method for eliminating background fluorescence is to subtract a background image from the raw image. The background image could be the cluster image obtained either before cluster formation or after cluster disappearance. However, this method is not applicable in our experiments because the background varied in time due to drifts in the TIRF illumination pattern and intensity, variations in autofluorescence as the cells grow, and debris floating into the area of observation. However, background fluorescence could be estimated from within the cluster image by use of a custom Fortran program for the 486 PC. When a cluster was identified by the user as displayed on the PC's VGA monitor, it could be enclosed by a rectangle via mouse control. Background intensities for the cluster could then be estimated by the average intensities of the neighboring pixels surrounding the rectangle.

After cluster identification, background estimation, image resizing to fit the CCD aspect ratio to that of standard video, and caption addition (all done on the PC with a custom Fortran program), the cluster images, together with the cell images, were transferred through ethernet onto a DEC-station (Color DECstation 5000/200 GPX Turbo) where the rest of the image processing was then performed.

With a Fortran program written on the DEC station, the raw cluster intensities were corrected by background intensity subtraction, scaled to the background intensities, and normalized to unity for each experiment. The subtraction and scaling were performed using the following rules to preserve the shapes of clusters, which would otherwise be smeared by the residual intensity of a direct subtraction because of the fluctuations arising from the white noise in both cluster and background intensities: if the intensity was ≥ 1.3 times the background intensity, the intensity was a ratio of the raw cluster intensity subtracting the background over the background; otherwise, the intensity was set to zero. Even though these rules somewhat over-estimated the background, they succeeded in producing a rather noise-free cluster image. The new cluster intensities were later displayed linearly with 15 colors using Utah Raster Toolkits (URT) subroutines on a Stardent ST1000 graphics supercomputer, which has a 24 bit graphic ability and is connected to the video recording equipment. Finally, using URT graphics, the processed pseudocolor cluster image was overlaid on top of the cell image. Our custom software for image acquisition and processing is not "user-friendly" but it is available upon request.

Video Recording and Editing

Since the Stardent digital graphic display format (RGB) is incompatible with the analog video display format (VHS or S-VHS), recording of the computer graphic displays onto a videotape requires the conversion of signal format from RGB into video. This conversion was accomplished using a RTC Scan Converter which input RGB from the Stardent ST1000 and output Super VHS (S-VHS) to a S-VHS Panasonic video recorder.

After being converted into S-VHS, each of the overlaid images was recorded as 3 successive frames (or 6 frames for just one experiment) on a S-VHS video tape, by utilization of a software-controllable Minivas system which monitored the video recording of the Stardent graphics. The Minivas was connected to the Stardent ST1000, the RTC Scan Converter, and the S-VHS Panasonic video recorder.

The final video editing was performed through a software-controllable Digital F/X system connected to a Macintosh computer. These steps included rearranging segments of the selected source video, inserting and overlaying graphics, fading in and out, and duplicating.

Still Images

For some experiments, "still" images rather than video sequences were gathered for the purpose of judging the frequency by which AChR clusters occur at cell-substrate contacts. These experiments compared cluster distribution as seen by TIRF vs. that seen by

TABLE 1. Cluster Location Summary[a]

No. of clusters	6 days	7 days
Total	200	150
At substrate contact regions	197	147
Partially at substrate contact regions	2	2
Not at substrate contact regions	1	1

[a]Day = 0 is set when cells were plated.

standard "trans-" (or "epi-") illumination. Rat muscle cells were first plated on coverglasses in Petri dishes and were grown at 37°C in an incubator for 6–7 days. They were then labeled with 4 μg/ml of R-BT in 1 ml HBSS buffer solution for 30 min at room temperature, after which the labeling solution was rinsed off 3 times with HBSS solution. Finally, these cells on the cover glass were mounted into a cell chamber (Bellco Glass Co., Vineland, NJ); basically a sandwich of two coverslips separated by a neoprene ring spacer) filled with HBSS for immediate observation with a Nikon 20×, 0.8 NA, glycerin-immersion objective on the microscope stage (Leitz Ortholux II). Observation was made with both epi-illumination by a defocused laser beam, and TIRF by a focused laser beam through the trapezoidal prism as described above.

RESULTS

Two sets of experiments were performed with distinct goals, as follows. (1) An investigation of the cluster locations relative to the myotube-substrate contact regions. This set involved still images, not a time-lapse video, but it was needed to verify whether TIRF illumination would observe a representative sample of the AChR clusters. (2) A time-lapse TIRF video study of the cluster images, including the time course of the cluster image intensity, the cluster lifetime, the correlation of this lifetime with its maximum intensity, and the locations and times of the first appearance of clusters.

Clusters and Cell-Substrate Contact Regions

On cultured rat myotubes, clusters form primarily at the substrate contact regions and, reportedly, to a lesser extent elsewhere (Bloch, 1986). The substrate contact clusters have been estimated to occupy about 65% of the substrate contact area (Bloch and Geiger, 1980). The experiments described in this section were designed to check and extend these observations because the TIRF illumination to be used in the time lapse video production can only "see" clusters (or parts thereof) at cell-substrate contacts. [Nevertheless, virtually all of the AChR in clusters should be accessible to labeling by R-BT because these AChR are generally not in the regions of extreme closest apposition to the substrate (Bloch and Geiger, 1980; Axelrod, 1980).] The clusters were observed as still images by alternating epi-fluorescence and TIRF. While epi-fluorescence

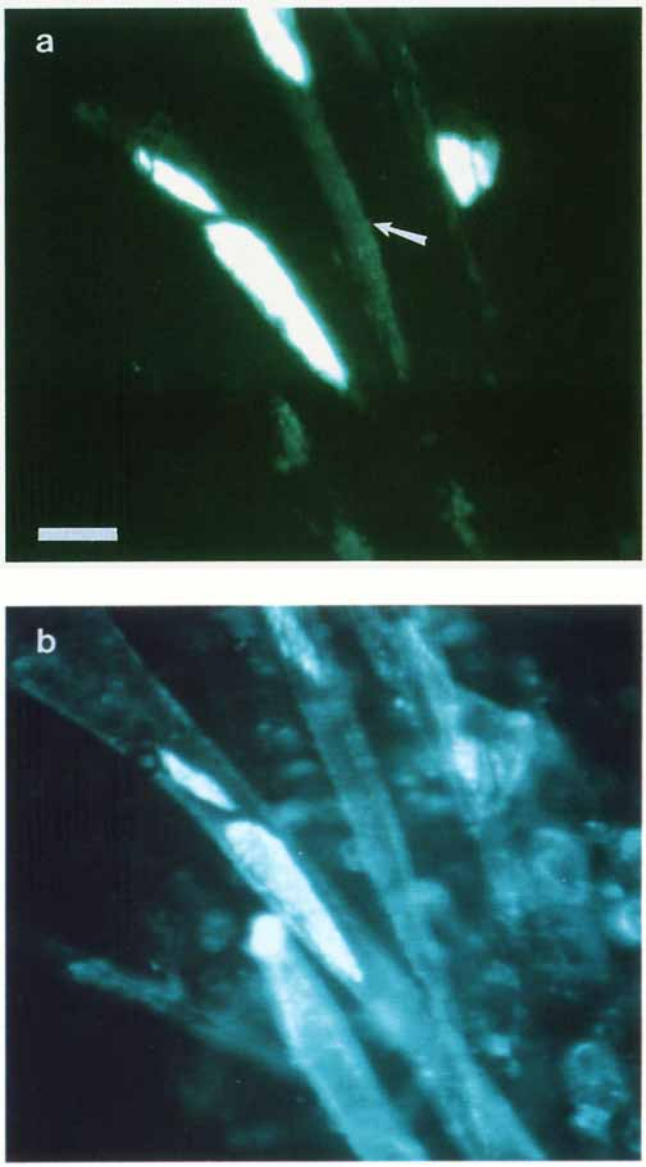

Fig. 4. Clusters viewed by a 20×, 0.8NA, glycerin immersion objective (Nikon). (**a**) TIRF image. The brightest regions are AChR clusters at the substrate contact regions, and the dimmer but still visible regions (marked by arrow) are nonclustered AChRs on the myotube membranes at substrate contact regions. (**b**) Epi-illumination image of the same area. The image shows the locations of myotubes as well as the clusters. The bright spot located at the upper tip of the lower myotube is simply fluorescent debris that appears in epi-illumination but not in TIRF; epi-illumination images are often confounded by autofluorescence of cells and fluorescent debris. Bar = 20 μm.

Fig. 5. A short sequence of selected video frames, displayed on a VGA monitor. In particular, these sequences show the lifetime of an indicated cluster. The location of this cluster is traced by an arrow, and the time after its appearance is (**a**) t = −0.8 hr (before its appearance), (**b**) t = 0.8 hr, (**c**) t = 2.5 hr, (**d**) t = 7.5 hr, (**e**) t = 14.2 hr, (**f**) t = 24.2 hr, (**g**) t = 29.2 hr, and (**h**) t = 34.2 hr. Bar = 100 μm.

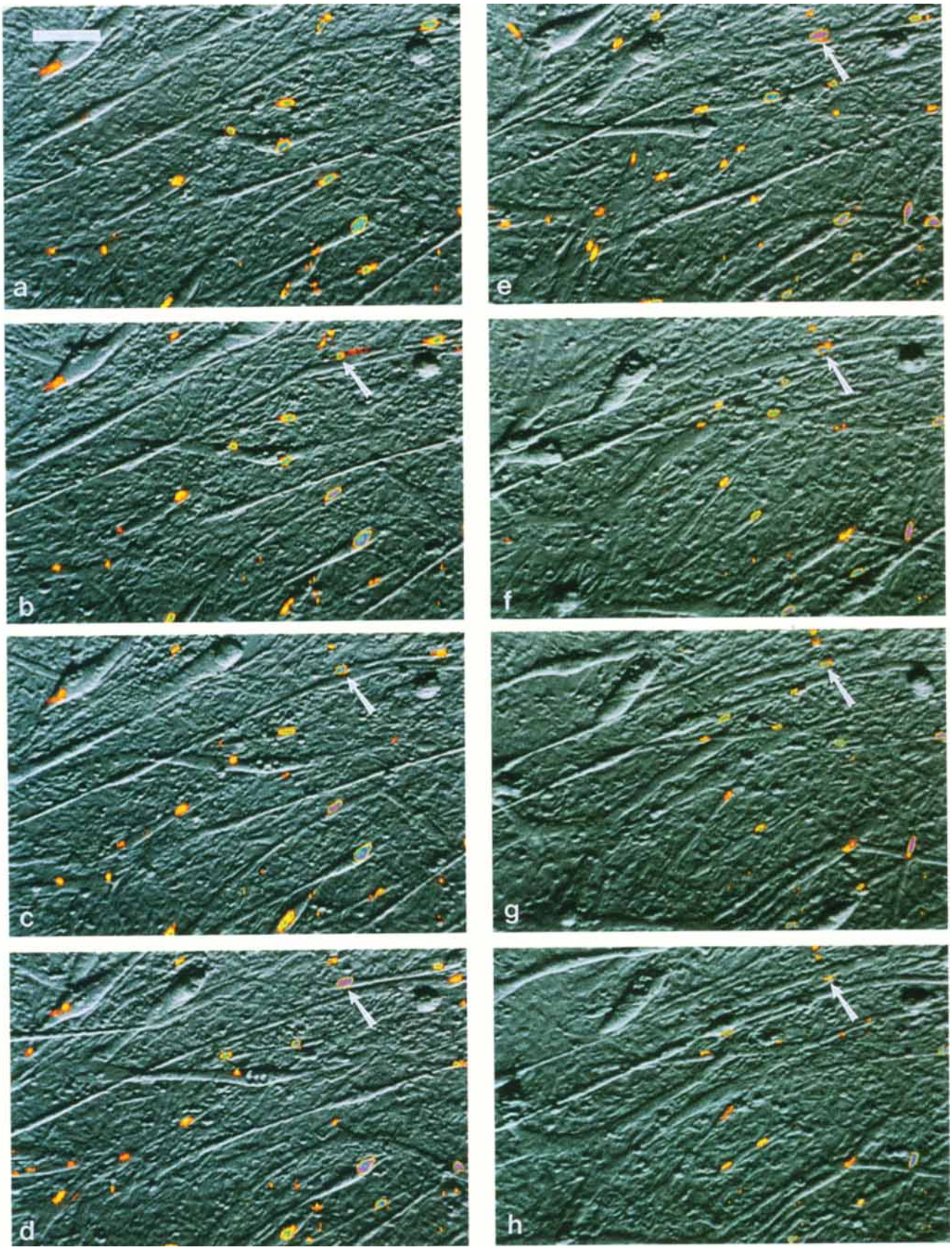

Fig. 5.

reveals clusters at all depths by varying the focus, TIRF only reveals clusters at the substrate contact regions. We address two questions: what fraction of clusters form at substrate contact regions; and what fraction of substrate contact areas have clusters?

Fraction of clusters present at cell-substrate contacts. A cluster can be classified into three categories according to its location relative to a cell-substrate contact region: (1) entirely at a contact region, (2) partially at a contact region, and (3) not at a contact region at all. The results of the experiment are summarized in Table 1. This table shows that > 97% of the clusters were located entirely at contact regions, and at most 3% of the clusters were either partially located at the regions or in the bulk. Even these 3% of the clusters had an abnormal morphology, appearing almost indistinguishable from fluorescent debris. Therefore the time-lapse movies made using TIRF reveal almost all of the existing clusters.

Fraction of cell-substrate contacts containing clusters. AChRs exist on myotube membranes both in the cluster regions with high density (about 5,000–8,000/μm^2), and in noncluster regions with lower density (about 1,000–1,500/μm^2) (Axelrod et al., 1976). When observed by TIRF illumination, the clustered regions appear bright with an intricate internal structure of microaggegates, often semi-ordered in paracrystalline arrays (Wang and Axelrod, 1994). The nonclustered regions also show some fluorescence (brighter than the dark background) at regions where the membrane was in close proximity to the substrate but it is much dimmer and more homogeneous than fluorescence in clusters (see Fig. 4). The total cell-substrate contact area could then be calculated as the sum area in those two types of regions. (A third type of fluorescence, cellular autofluorescence, is negligibly dim in TIRF compared to R-BT labeled AChR, and in direct color viewing through appropriate microscope barrier filters, appears somewhat more orange than the yellow tint of rhodamine.)

Cultures at 7 days after plating were used for these measurements. Images were recorded at random positions on the sample. From these images, the total area occupied by the cell-substrate contact regions and the total area occupied by the clusters were then calculated. Our calculation shows that only 25% of the contact regions (defined as close enough to be within the TIR evanescent field) were occupied by clusters, significantly less than the 65% estimated by Bloch and Geiger (1980) by use of interference reflection microscopy in conjunction with epi-fluorescence and phase contrast optics. The reason for the discrpancy is not clear. Perhaps TIRF more sensitively detects cell-substrate contact regions because of its inherent higher contrast than interference reflection optics. Alternatively, perhaps a subtle effect of substrate surface charge, nutrient medium, or sample fixation (used in the Bloch and Geiger experiments) accounts for the difference.

TABLE 2. Video Details of the Six Experiments

	Experiment					
	1	2	3	4	5	6
Total no. of days[a]	7.0	7.4	7.0	5.9	8.3	6.2
Time between observations (min)	20	20	20	60	20	20
No. of bleachings	0	0	0	0	2	3
No. of video frames/picture	3	3	3	6	3	3
Movie duration (sec)	35.5	45.3	40.0	23.3	36.5	29.0
Magnification (no. of pixels/100 μm)	55	55	55	84	55	55

[a]Day = 0 is set when cells were plated.

Time-Lapse Development of Clusters

Six separate culture dishes were the subjects for time-lapse movies, the optical and video details of which are shown in Table 2. Note that experiments 5 and 6 included "bleaching" pulses. These were occasional periods of TIR laser illumination of long duration on the order of tens of minutes rather than the brief 1 sec used for recording images. This treatment irreversibly photobleaches all of the labeled AChRs within the TIR evanescent field, thereby obliterating fluorescence from preexisting AChRs. However, AChRs which are subsequently incorporated into the cell surface and become labeled by the continuous presence of R-BT (or AChRs that diffuse into the evanescent field from more distal regions of the cell membrane) can be seen in post-bleach images.

Each movie (VHS copies of which are available upon request) condenses a week-long experiment to less than a minute. They show the processes of the myoblast fusion into myotubes and the formation and disappearance of AChR clusters. A short sequence of the selected video frames in Figure 5 a–h shows the life history of a particular cluster. The cluster first emerges on one of the myotubes with low cluster density. It then matures rapidly by increasing its size and density in about 6 hr. Once formed, its size and density stay relatively invariant for about 13 hr followed by its gradual disappearance in about 12 hr. Notice that the position of the cluster changes very slightly compared to that of the myotubes, shown in gray-scale schlieren optics. The changes in the AChR cluster size and density are easily visualized with pseudocolors.

To quantify some of the salient features of cluster behavior, several quantitative plots based on pixel intensities (defined as the ratio of the original pixel intensity after background subtraction to the background intensity) are used, all derived by custom Fortran programs.

Number of clustered AChRs vs. time. Figures 6a–d and 7a–b are plots of total cluster image intensity vs. time for the six dishes. The total cluster image intensity is defined as the summation of the intensity scaled to its background intensity from each pixel enclosed in all the rectangles that delimit each cluster in

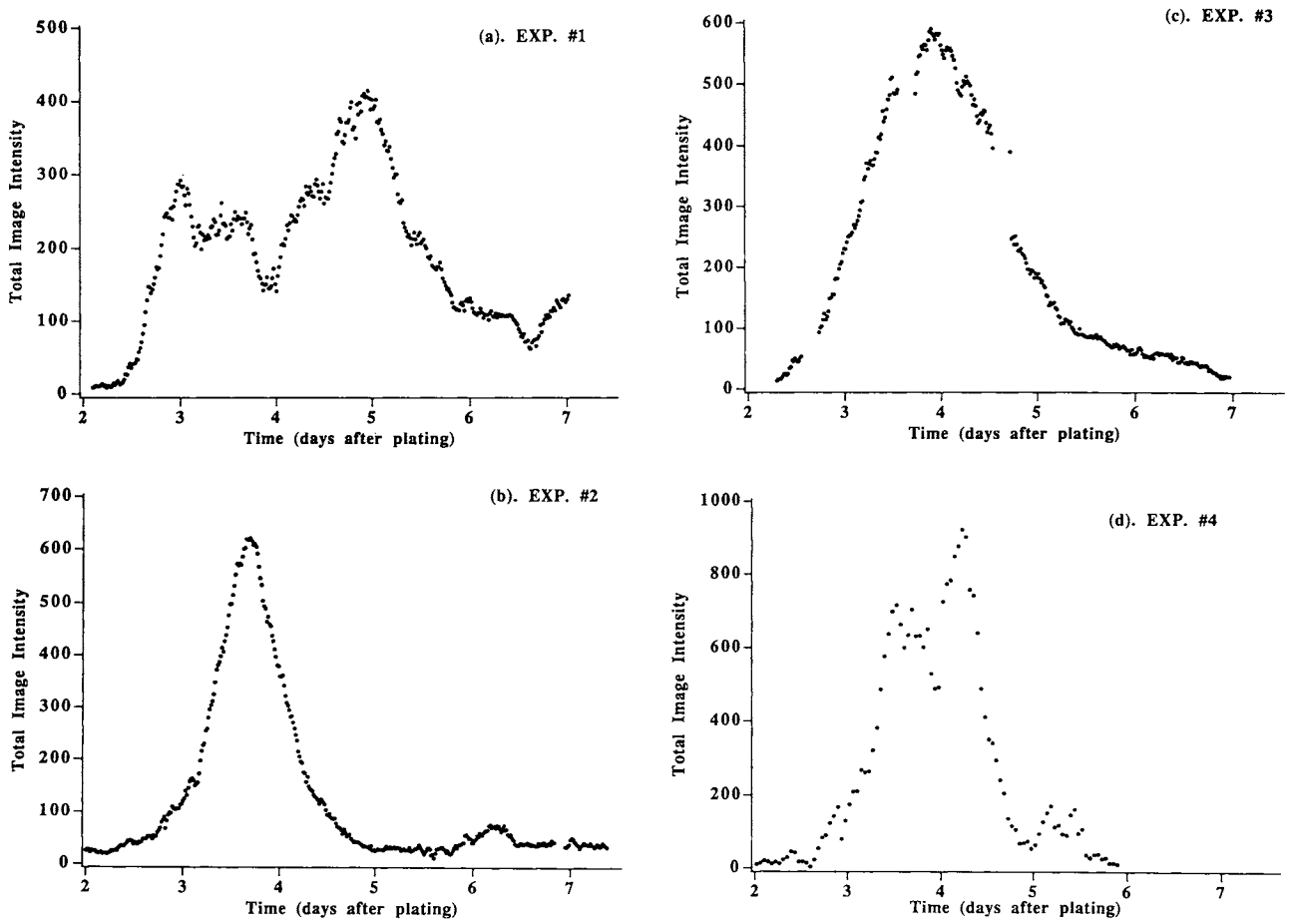

Fig. 6. The time course of the total cluster image intensity in the four experiments without photobleaching pulses, showing that clusters can be found on the cultures within a time window of about 3 days.

the image and is therefore proportional to the total number of clustered AChRs present in the image. All these plots show that clusters can be found in the cultures during a time window of about 3 days duration. Figure 7a,b in particular represent the dishes subjected to photobleaching bursts as indicated. They show that newly incorporated or migrated AChRs are constantly forming new clusters or being incorporated into pre-existing clusters: after photobleaching, total fluorescence intensity in clusters often recovers within a few hours. However, some clusters, particularly those on older cultures, do not regain their fluorescence after photobleaching (e.g., the response to the last bleach on Fig. 7a).

Single cluster intensity vs. time. Splitting and merging of clusters are occasionally observed. Figure 8 is the time course of a particular single cluster intensity with the cluster shape schematically indicated on the top of the curve at different times. The cluster intensity is defined as the summation of the intensity scaled to its background intensity from each pixel enclosed in the rectangle that delimits the cluster in the image and is therefore proportional to the total number of clustered AChRs present in that cluster. This cluster emerged on the third day after plating, and disappeared about 2 days later. During this time, a smaller cluster split from and later merged into the pre-existing cluster.

Distribution of cluster lifetimes. The lifetime of a cluster is defined as the duration of time between a cluster intensity rising and dropping to 5% of its maximum intensity. Figure 9 shows that the average lifetime of a typical individual cluster is only about 1 day.

Maximum intensity of a cluster vs. its lifetime. Figure 10 shows the correlation between the maximum intensity of a cluster and its lifetime (i.e., the time duration during which the intensity is greater than the threshold value). This plot indicates that the larger and brighter clusters tend to be longer-lived. Some of this apparent effect may be due to our thresholding criterion of counting only clusters with a fluorescence intensity greater than 1.3 times the background intensity.

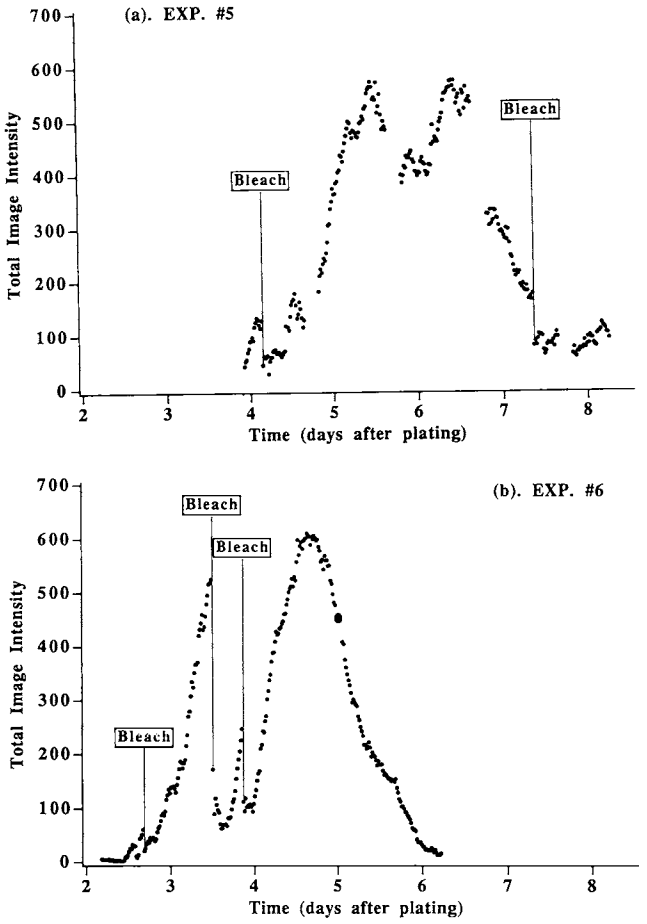

Fig. 7. Rate of the incorporation of AChRs into clusters. These are two photobleaching experiments that show that fresh AChRs are constantly forming new clusters or being re-incorporated into pre-existing clusters: after photobleaching, total fluorescence intensity in clusters recovers within a few hours to its prebleach level.

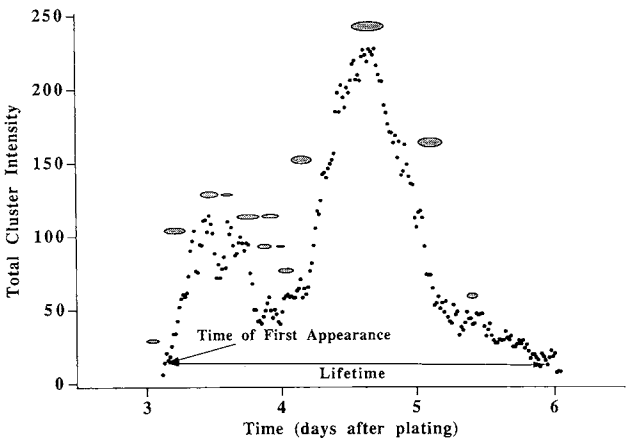

Fig. 8. The time course of a single cluster intensity. The shape of the cluster is schematically indicated on top of the curve. Splitting and merging of clusters were occasionally observed. This figure also shows the definitions of the cluster lifetime and the time of the first appearance. The cluster lifetime is defined as the time between the intensity of the cluster rising to 5% of its maximum and dropping to 5% of its maximum. The time of the first appearance is defined as the time when the cluster intensity rises to 5% of its maximum.

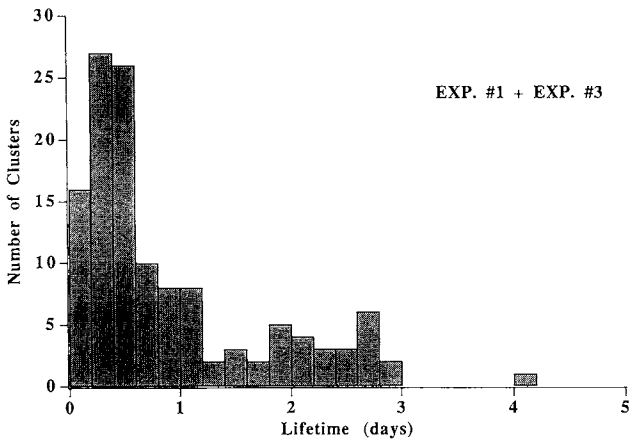

Fig. 9. Distribution of cluster lifetimes. This shows the expected lifetime of a typical individual cluster is very short, about 1 day or less.

Distribution of first appearance time of a cluster. The time of first appearance of a cluster is defined here as the time (after plating) at which the intensity of a cluster rises up to 5% of its eventual maximum intensity. Figure 11 shows the distribution of the times of the first appearance of a cluster. As evident from the figure, there is a sudden, almost synchronous initial appearance of numerous clusters at around 2.5 days.

DISCUSSION

We report here the first time-lapse movies produced with TIRF illumination. TIRF with CCD detection has several desirable features for making such movies which previously have not been available, as follows.

1. Since TIRF illuminates only cell-substrate contact regions where almost all of the AChR clusters are located, cluster images show very little background from the cellular autofluorescence. The TIR-excited autofluorescence in myotubes contributes an intensity equivalent to no more than a few hundred rhodamine fluorophores per μm^2. Combined with the full efficiency of light gathering in TIRF microscopy (as opposed to confocal systems) and the high sensitivity of the CCD camera, the negligible autofluorescence allows very low fluorophore surface concentrations (less than $1{,}000/\mu m^2$) to be recorded.

2. Fluorophores can be continuously present in the medium without obscuring the image. In our case, this allows immediate and continuing labeling of receptors newly incorporated into the membrane by R-BT. In other biological systems, this same feature would allow visualization of receptors at the contact regions that bind only reversibly to fluorescence-labeled ligands.

3. Fluorescence from receptors which have become

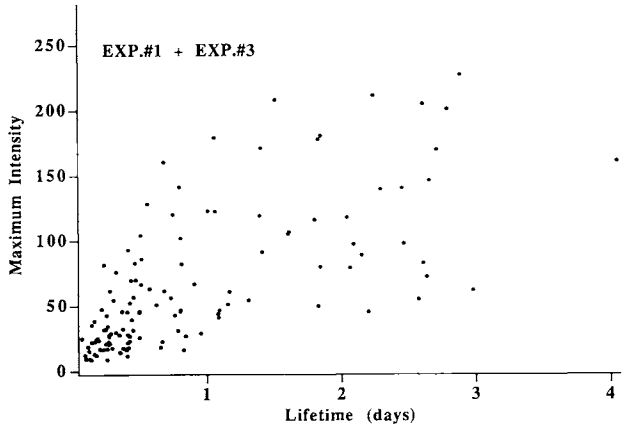

Fig. 10. Correlation between a cluster's maximum intensity and its lifetime, indicating that the largest and brightest clusters tend to be longer-lived.

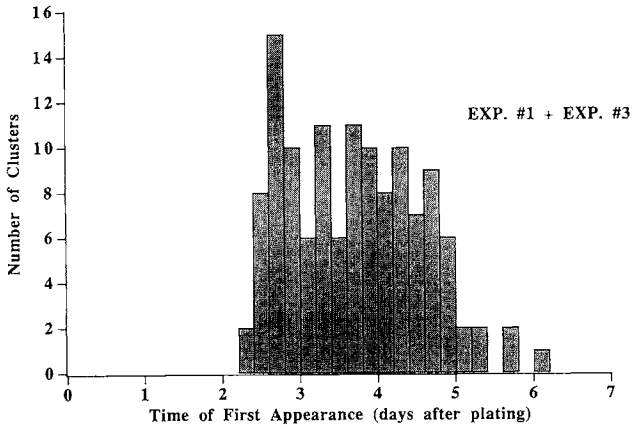

Fig. 11. Distribution of the times of the first appearance. The initial appearance of numerous clusters is rather sudden.

internalized is not excited with TIRF illumination. In standard epi-illumination, even a receptor turnover time of 10–20 hr [as for the AChR; see Axelrod (1980)] would preclude long-term observation of a cell culture.

4. As an optical sectioning technique, TIRF exhibits some advantages and disadvantages relative to confocal microscopy (CM) for producing time-lapse sequences. CM is more versatile in that it can optically section any plane, not just the cell-substrate contact plane. But TIRF excites (and gathers) fluorescence from a layer of only 0.1 μm thickness; CM excites the entire depth of the cell and gathers fluorescence effectively from a considerably thicker layer (about 0.6 μm). Also in practice, the efficiency of fluorescence throughput for TIRF is much higher than for CM. These features mean that TIRF requires less excitation light over less of the cell's bulk volume to visualize a brighter image. TIRF thereby is less likely to damage the cell by photochemical reactions during long-term viewing experiments. We have observed in the past that epi-illumination at a level and frequency necessary to make movies suppresses the local appearance of AChR clusters, reduces the number of myotubes under view, and adversely affects their morphology (unpublished observations).

5. The image detection by a high sensitivity CCD camera allowed recording of a more complete time sequence than previously possible by standard photography while still avoiding irreversible photobleaching. The digital output also lends itself to pseudocoloring and multiple image overlaying.

6. By use of a custom-designed chamber, cell cultures could be maintained alive and observed by TIRF on the microscope stage through the entire 7-day period, in the same dish in which the cells were plated.

Aside from highlighting the technical features of TIRF, these time-lapse video sequences overlaying TIRF and schlieren illumination, along with the associated analyses of still frames, tend to confirm, extend, and quantify observations on AChR clusters on rat myotubes made by previous studies, notably those of Bloch and collaborators (Bloch, 1979, 1986; Bloch and Geiger, 1980; Bloch and Pumplin, 1988; Bloch et al., 1989). These biological conclusions are as follows:

1. Clusters are induced by myotube-substrate contacts but not by myotube-myotube contacts. These substrate contact-induced clusters account for at least 97% of all clusters. Clusters appear only after myoblasts fuse to form myotubes. Clusters remain at the contact regions during their lifetime and move very slowly relative to myotube motion. Among the substrate contact regions, AChR clusters in our preparations occupy only about 1/4 of the contact area, somewhat less than the 65% previously observed by Bloch and Geiger (1980).

2. The initial wave of cluster formation tends to occur nearly synchronously on many myotubes. No clusters are seen on mononucleated myoblasts. "Young" myotubes—those just formed by fusion from myoblasts—rarely have more than one cluster.

3. The average lifetime of an individual cluster is only around 1 day, although [as previously noted by Bloch (1979)], clusters are generally present in cultures for about 3 days. The largest and brightest clusters tend to be longer-lived.

4. New AChRs continuously appear in some pre-existing clusters: after photobleaching, the fluorescence of some clusters recovers within a couple of hours, whereas that of others never recovers. Perhaps the inevitable disappearance of each cluster may be due to a shutdown of new incorporation while an ongoing removal of preexisting receptors continues apace. It is also possible that some of the fluorescence that reappears in photobleached samples migrates into the evanescent field from cell surface regions farther away from the substrate. It is known (Stya and Axelrod, 1983) that nonclustered AChR can indeed become incorporated into clusters. But given the rather slow dif-

fusion rate of a nonclustered AChR (10^{-10} cm^2/sec) and a typical lateral distance a nonclustered AChR needs to traverse toward a cluster (20 μm), it seems that lateral diffusion would not account for all of the new AChRs in pre-existing clusters. At least some of the postbleach restoration of fluorescence likely arises from AChRs newly incorporated into the membrane from the interior.

The TIRF/time-lapse methods presented here can be used for other studies on AChR clusters, including: (1) the effects of drugs, including disaggregating agents of clusters such as carbachol and cytochalasin, and inhibitory agents of clusters such as colchicine; (2) the correlation between AChR clusters and cytoplasmic elements using fluorescent antibodies to cytoplasmic elements or fluorescent analogs of cytoplasmic elements; and (3) the time course study of cluster patterns at high magnification. Apart from studies on cell surface AChRs, these methods can also be extended to make time-lapse movies of: (1) cell motility, where cell membranes are first fluorescently labeled, and the substrate-contact regions are then observed with TIRF; and (2) cell surface components that specifically aggregate at contact regions with substrates that have been derivatized with specific complimentary molecules such as antibodies, antigens, lectins, or cell adhesion molecules.

ACKNOWLEDGMENTS

The authors thank Ms. Sharada Kumar for cell culture preparation, Mr. Keith Shaw for his help in electronics circuitry design, Dr. Robert M. Fulbright for his generous help in computer programming and laboratory equipment operations, Drs. Kate Barald and Richard Neubig for their useful comments, and the Computer Aided Engineering Network staff at the University of Michigan School of Engineering (especially Dr. Amadi O. Nwankpa and Mr. Curt Malouin) for their assistance in using the CAEN network. This work was supported by NIH NS 14565 and NSF DMB 8805296.

REFERENCES

Axelrod, D. (1980) Cross-linkage and visualization of acetylcholine receptors on myotubes with biotinylated α-bungarotoxin and fluorescent avidin. Proc. Natl. Acad. Sci. U.S.A. 77:4823–4827.

Axelrod, D. (1981) Zero-cost modification of bright field microscopes for imaging phase gradient on cells: Schlieren optics. Cell Biophys. 3:167–173.

Axelrod, D., Ravdin P., Koppel, D.E., Schlessinger, J., Webb, W.W., Elson, E.L., and Podleski, T.R. (1976) Lateral motion of fluorescently labeled acetylcholine receptors in membranes of developing muscle fibers. Proc. Natl. Acad. Sci. U.S.A. 73:4594–4598.

Axelrod, D., Burghardt, T.P., and Thompson, N.L. (1984) Total internal reflection fluorescence. Ann. Rev. Biophys. Bioengin. 13:247–68.

Axelrod, D., Hellen, E.H., and Fulbright, R.M. (1992) Total internal reflection fluorescence. In: "Topics in Fluorescence Spectroscopy, Vol. 3: Biochemical Applications," Lakowitz, J.L. (ed). New York: Plenum Press, pp 289–343.

Bloch, R.J. (1979) Dispersal and reformation of acetylcholine receptor clusters of cultured rat myotubes treated with inhibitors of energy metabolism. J. Cell Biol. 82:626–643.

Bloch, R.J. (1986) Loss of acetylcholine receptor clusters induced by treatment of cultured rat myotubes with carbachol. J. Neurosci. 6:691–700.

Bloch, R.J., and Geiger, B. (1980) The localization of acetylcholine receptor clusters in areas of cell-substrate contact in cultures of rat myotubes. Cell 21:25–35.

Bloch, R.J., and Pumplin, D.W. (1988) Molecular events in synaptogenesis: Nerve-muscle adhesion and postsynaptic differentiation. Am. J. Physiol. 254:C345–C364.

Bloch, R.J., Velez, M., Krikorian, J.G., and Axelrod, D. (1989) Microfilaments and actin-associated proteins at sites of membrane-substrate attachment within acetylcholine receptors clusters. Exp. Cell Res. 182:583–596.

Changeux, J.P. (1989) The acetylcholine receptor: Its molecular biology and biotechnological prospects. BioEssay 10:48–54.

Changeux, J.P., Fontaine, B., Klarsfled, A., R., Laufer, R., and Cartaud, J. (1989) Molecular biology of acetylcholine receptor long-term evolution during motor end-plate morphogenesis. Prog. Brain Res. 79:15–25.

Froehner, S.C. (1991) The submembrane machinery for nicotinic acetylcholine receptor clustering. J. Cell Biol. 114:1–7.

Haest, C.W.M. (1982) Interactions between membrane skeleton proteins and the intrinsic domain of the erythrocyte membrane. Biochim. Biophys. Acta 694:331–352.

Krikorian J.G., Daniels, M.P. (1989) Reorganization and stabilization of acetylcholine receptor aggregates on rat myotubes. Dev. Biol. 131:524–538.

Kuromi, H. (1987) Mechanism of acetylcholine receptor accumulation at the nerve-muscle junction during development. Asia Pacific J. Pharmacol. 2:195–202.

Olek, A.J., Krikorian, J.G., and Daniels, M.P. (1986) Early stages in the formation and stabilization of acetylcholine receptor aggregates on cultured myotubes: Sensitivity to temperature and azide. Dev. Biol. 117:24–34.

Ravdin, P., and Axelrod, D. (1977) Fluorescent tetramethyl rhodamine derivatives of α-bungarotoxin: Preparation, separation, and characterization. Anal. Biochem. 80:585–592 and erratum 83:336.

Stya, M., and Axelrod, D. (1983) Diffusely distributed acetylcholine receptors can participate in cluster formation on cultured rat myotubes. Proc. Natl. Acad. Sci. U.S.A. 80:449–453.

Wang, D., and Axelrod, D. (1994) Microclustering patterns of acetylcholine receptors on myotubes studied by spatial fluorescence autocorrelation. Bioimaging 2:22–35.